Pakistan Journal of Engineering and Technology
ISSN (Print): 2664-2042; ISSN (Online): 2664-2050
Received: 2024-09-14
Accepted: 2025-02-27
https://doi.org/10.51846/vol8iss1pp40-46

PAKJET
Pakistan Journal of Engineering & Technology

Article

Investigating the Effect of Injection Start Time in Compression Ignition Engine: A Reactive Control on Waste Heat Recovery Capacity

Hamed Asghari, and Amin Farzin *

Department of Mechanical Engineering, Islamic Azad University, Langarud Branch, Guilan, Iran
* Correspondence: Amin Farzin (amin.farzin@iau.ac.ir)

Abstract: Approximately one-third of the energy supplied to the cylinder of an internal combustion engine is transformed into effective work, while the remaining energy is dissipated in multiple ways. Offering solutions that can recuperate some of the energy the engine wastes is important and beneficial. This research examines how the timing of injection start influences the ability to reclaim waste heat in a reactive control compression ignition engine. Following the validation, the diesel fuel injection timing was adjusted. Their effects on exergy destruction, productivity coefficient, engine output power, and produced pollutants have been studied. The results showed that by advancing the start time of fuel injection, parameters such as the efficiency of the first law of thermodynamics and pollutants such as unburned hydrocarbons and carbon monoxide increased and decreased, respectively. In addition, the exergy resulting from the heat transfer has increased due to the high heat transfer due to the high temperature of the load inside the cylinder. Therefore, the high temperature has caused the irreversibility to increase due to the increase in the number of chemical reactions. The efficiency of the system increased with advanced fuel injection start time.

Keywords: Injection Start Time, Compression Ignition Engine, Reactive Control, Waste Heat Recovery

1. Introduction

Internal combustion engines are commonly utilized for generating power as well as for heating and cooling processes. [1]. A big part of the energy derived from fuel-air burning is not used to create work. It is instead put to the environment through cold air and exhaust fumes. Consequently, transforming the waste heat from internal combustion engines into valuable work contributes to effective energy management [2]-[4].

A team of researchers utilized exhaust gases from diesel engines to operate the absorption refrigeration unit. From the findings, it is evident that the arrangement of the cycle and the parameters of performance play a role in both fuel consumption and the efficiency of the system. [5]-[7]. Abusoglu et al. analyzed a system that produces heat and electricity simultaneously, utilizing a diesel engine by the first and second laws of thermodynamics. They determined the exergy loss associated with each component of the system [8]. Srinivasan and colleagues explored the possibilities of recovering waste heat from the emissions of a highly efficient dual combustion engine through the use of a Rankine cycle [9]. Several groups have reported their findings on using ORC to recover waste heat from diesel engines that are powered by various fuels and under different conditions [10]-[13]. Furthermore, other researchers performed a similar analysis using a submarine diesel engine [12], [14]. Emin Açıkkalp and his colleagues performed a progressed exergoeconomic study of a trigeneration system driven by a diesel-gas engine. It was found in the study that the combustion chamber, high-pressure steam turbine, and condenser can greatly benefit from reduced exergy usage due to their high cost of exergy destruction [15]. With the rise of low-temperature combustion (LTC), the concept of employing these engines was also contemplated in concurrent production processes [16]-[18]. Using the heat from the exhaust of a homogeneous mixture compression ignition engine, Sarabchi et al. powered a steam-driven power cycle, an air conditioning system and a desalination system [19]. In their study, Khaljani and the research group used the waste heat from the cooling water and the exhaust gases of their engine to operate two Rankine cycles [20]. It is an internal combustion engine based on the concept of low-temperature reactions. In this process, two different fuels are used together. The first test has a low reactivity value, while the second has a high reactivity. The low reactivity fuel is added in a predictable way into the engine combustion chamber together with the air from the inlet, while the high reactivity fuel gets injected by the injector into the chamber [21]-[23].

In the past few years, researchers have shown increasing interest in reactive control compression combustion engines, leading to numerous studies aimed at enhancing these engines. Several investigations have explored how different parameters of reactive control combustion engines influence the performance of refiners [21]-[23]. Since the reactive control compression combustion engine has the advantage of low emissions and high fuel consumption efficiency, this engine can be used in simultaneous production cycles [21]. In the research performed by Liu et al., an analysis based on the first and second laws was conducted for three combustion modes of a conventional diesel engine: homogeneous mixture compression ignition, combustion, and reactive control compression ignition [24]. Factors such as in-cylinder temperature, the extent of chemical reactions, combustion temperature, reaction rates, and duration of combustion have been found to be key contributors to such loss of exergy. Based on the results, the highest level of exergy destruction was found in the conventional diesel engine [25]. In a different study carried out by Li et al., the influence of methanol and gasoline on the exergy loss in a reactive control compression combustion engine was examined utilizing a multidimensional model along with a simplified chemical kinetics mechanism. The findings from this research indicated that the use of diesel-methanol fuel leads to elevated combustion temperatures, resulting in greater exergy destruction during the chemical reactions [24]. Mohebbi and colleagues examined how exhaust gas recirculation and the incorporation of normal heptane into low reactivity fuel influence a reactive control compression combustion engine [26]. In this research, it was observed that as the recirculation of exhaust gases increased, the total exergy destruction also rose, and as a result of the lowered combustion temperature linked to the high heat absorption capability of the recirculated gases, thermomechanical exergy was reduced [26]. By raising the proportion of normal heptane above isooctane, known for its low reactivity as a fuel, the exergy of heat transfer has significantly improved. This enhancement in heat transfer can be attributed to the increased reactivity of the mixture resulting from the inclusion of normal heptane [26].

The primary objective of this research is to explore how the timing of fuel injection in a reactive control compression combustion engine, which uses a blend of natural gas and diesel, influences the capacity for waste heat recovery. To accomplish this aim, the engine is initially simulated with a three-dimensional model, and its performance is subsequently validated using experimental data. Additionally, various injection timings have been applied to the constructed model, and the impacts of these timings on waste heat recovery capacity have been assessed.

2. Materials and Methods

In this study, a three-dimensional engine model was employed for simulation. The model's accuracy was confirmed through experimental data, after which the timing of diesel fuel injection was modified to examine its impacts on exergy destruction, waste heat recovery potential, and exhaust power output.

2.1. Specifications of Selected Engine and Injector

The researchers used a 1.9-liter light engine from Volkswagen which is available at the Advanced Power Systems Research Center at Michigan Technological University. It runs on a 4-cylinder diesel, with the variable geometry turbo feature. Each cylinder was equipped with a diesel fuel injector manufactured by Bosch (CRDI). Table 1 provides the specifications for both the engine and the injector.

Table 1. Specifications of engine [27] and injector [28].

Title	Engine Characteristics	Title	Injector Characteristics
Model	TDI Volkswagen	The kind of injector	CRDI
Engine Displacement	1900 CC	Injector spray	Conical form
Number of cylinders	4	Spraying angle	144º
Cylinder Diameter	79.5mm	Pressure	400/bar
Compression ratio	17.1	Number of injector nozzles	6
Stroke	95.5 mm	The angle between the injector nozzles	60º
Before top dead center (BTDC)	169º		
After top dead center (ATDC)	162º		

2.2. Models and Simulations

Converge software was utilized to model the fluid dynamics and combustion phenomena taking place within the cylinder. The operational cycle of the engine was represented as a closed cycle, and when the intake valve was shut, the mixture within the cylinder was regarded as entirely homogeneous and uniform. Additionally, a simplified chemical mechanism comprising 76 species and 464 reactions was employed to replicate the combustion process [29].

The patterns used, such as droplet breaking, turbulence, heat transfer, etc., are shown in Table 2. In order to validate the simulation results, two operating modes for the engine have been considered according to Table 3.

2.3. Prediction of Cylinder Pressure and Heat Release Rate

The in-cylinder pressure and heat release rate were predicted using the Converge code and compared against experimental values collected for the Volkswagen engine at Michigan Technological University Fig. 1. The operating conditions are outlined in Table 3. The results from the numerical method align well with the experimental data. Additionally, the predictions of pollutants and their comparison with experimental data are shown in Table 4. All conclusions are drawn for mode a.

2.4. Analysis of the Second Law of Thermodynamics

When temperature, mechanical, and chemical equilibrium with the environment are reached in a system, the highest amount of useful work it can produce is known as efficiency [30]. Usually, the exergy of a closed system is found using equation (1). Equation (2) is used to calculate the lost exergy because of heat transfer. T in this equation refers to the average temperature of air inside the chamber and the temperature outside. The amount of heat loss is obtained by solving the governing equations.

Table 2. Utilized model in documented simulations.

Method Name	Method Type	Reference
Kelvin-Helmholtz Rayleigh-Taylor (KHRT)	spray breakup	[30]
Dynamic stretching model	Dynamic stretching	[31]
Negative temperature coefficient (NTC)	ignition delay times with rising temperature	[32]
O'Rourke	penetration rates and the drop size distributions	[33]
Wall film formation and vaporization	spray-wall impingement	[34]
RNG k-epsilon model	turbulence	[35]
Han and Reitz model	Temperature Wall Function	[36]

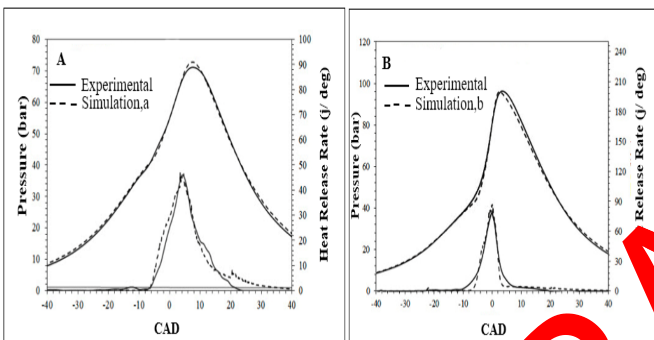

Figure 1. A chart illustrating the cylinder pressure (A) and Heat Release Rate (B) for both experimental and simulation scenarios according to the crank angle [28].

Table 3. Operating features of the ignition engine.

Parameters	a	b
Engine speed	1300	1500
Brake Mean Effective Pressure (bar)	4	5
Diesel fuel flow rate(gr/s)	0.071	0.107
Natural gas flow rate(gr/s)	50%	56%
Inlet airflow rate(kg/h)	60.7	59.95
Before top dead center (BTDC)	[illegible]	-55,20
IVC temperature (K)	348	378
Diesel spray pressure (bar)	400	400
Blend Ratio: Natural gas/Diesel	89	85
Refed gas	0	20%

Table 4. Compression and validation of pollutions in two tested forms.

Kinds of Pollution	A Form		B Form	
	Simulation	Experimental	Simulation	Experimental
Nitrogen oxides (ppm)	721	860	1738	680
Hydrocarbon (ppm)	4155	7800	3317	5300
Carbon monoxide (ppm)	636	1370	564	1100

$$\frac{dA}{d\theta} = \frac{dA_w}{d\theta} - \frac{dA_q}{d\theta} - \frac{\mathrm{dl}}{d\theta} + \frac{dA_{ch}}{d\theta} \quad (1)$$

$$\frac{dA_q}{d\theta} = \left(1 - \frac{T_0}{T}\right)\frac{dQ}{d\theta} \quad (2)$$

Equation (3) is used to calculate work exergy. Exergy of work is equal to the net work done, so it is obtained from the difference between the work done on the system and the work done on the environment.

$$\frac{dA_w}{d\theta} = (P - P_0)\frac{dV}{d\theta} \quad (3)$$

Equation (4) is used to calculate the chemical exergy changes of the mixture inside the combustion chamber. The chemical exergy changes of the mixture include the sum of the chemical exergy changes of the methane fuel and the exergy measurements of the diesel fuel. The chemical exergy changes of other types have been omitted due to their small amounts. The chemical exergy of the fuel is the maximum work produced as a result of burning the fuel and converting it into complete combustion products, including carbon dioxide and water. The equations used are as follows [37]-[39].

The sum of thermomechanical exergy and chemical exergy of the system is called the total exergy of a system. Thermomechanical exergy is the useful work of the system when it reaches the ambient temperature and pressure from the operating temperature and pressure. This state is called a limited dead state. Chemical exergy is the useful work of the system when the system reaches the common composition in the environment from its basic composition [37], [39].

$$\frac{dA_{ch}}{d\theta} = \left(\frac{dm_{ch}}{d\theta} \times a_{fv,CH4}\right) + \left(\frac{dm_{c,h16}}{d\theta} \times a_{fv,C,H16}\right) \quad (4)$$

$$a_{fv} = a_{fv,thermomechanical} + a_{fv,chemical} \quad (5)$$

$$a_{fv,thermomechanical} = h_{fv} - -T_0\, s_{fv} - g^0_{fv} \quad (6)$$

$$\begin{aligned} a_{fv,thermomechanical} &= g^0_{fv} - a g^0_{co2} \\ &- \left(\frac{\beta}{2}\right) g^0_{n2o}\left(a + \frac{\beta}{4} - \frac{\gamma}{2}\right) g^0_{o2} \\ &- RT_\theta In(z) \end{aligned} \quad (7)$$

$$Z = \frac{a^{a(\frac{\beta}{2})^{\frac{\beta}{2}}}\,\delta^{\delta}}{\sigma^{\sigma(a+\frac{\beta}{4}-\frac{\gamma}{2})^{(a+\frac{\beta}{4})-\frac{\gamma}{2})}}} \quad (8)$$

$$\varepsilon = \frac{\left(a + \frac{\beta}{4} - \frac{\gamma}{2}\right)}{0.21} \quad (9)$$

$$\sigma = 0.79_{\varepsilon} + a + \frac{\beta}{2} \quad (10)$$

Equation (11) was used to calculate thermomechanical exergy.

$$A_{tm} = (U - U^0) + P_0(V - V^0) - T_0(S - S^0) \qquad (11)$$

3. Results and Discussion

Fig. 2 shows the average pressure (Fig. 2A) and temperature (Fig. 2B) of the fluid inside the combustion chamber for different injection times. According to Fig. 2, it is clear that in the case that the injection start time is 25 degrees before the top dead point, the highest pressure and temperature are obtained inside the combustion chamber, and this result can be seen that by choosing the diesel fuel injection start time at 5 degrees Before the top dead point, the lowest temperature is created inside the combustion chamber. These results are caused by the temperature inside the cylinder at the time of combustion due to the different durations of mixing fuel with air in different conditions .Furthermore, the temperature at the injection start time, 25, 35 and 20 before the dead point has reached the maximum, and the reason for this occurrence is that there is more time for fuel and air to mix as well as possible at the early fuel injection start time, which causes combustion with high temperature. Increased and as a result the fuel burns more completely, these results are shown in Fig. 3. In addition, by delaying the fuel injection because the fuel-air mixing time is reduced, the fuel is incompletely burned as shown in Fig. 3 and finally the combustion temperature is reduced.

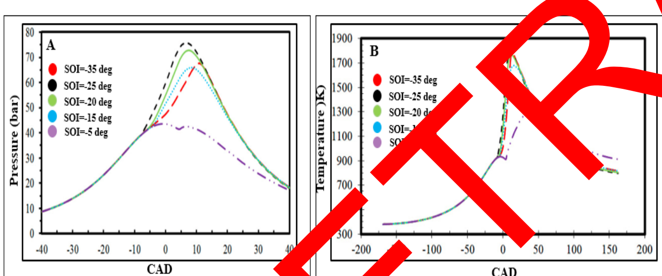

Figure 2. Illustration of the start injection timing (SOI) role on Pressure (A) and Temperature (B).

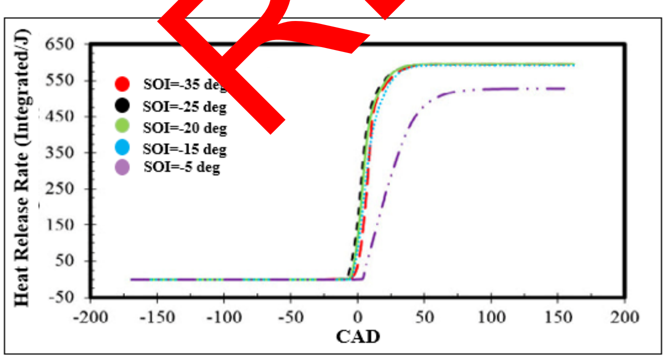

Figure 3. Illustration of the effects of start of injection timing on Integrated Heat Release Rate (IHRR).

Fig. 4A shows the exergy resulting from heat transfer. Based on the graph, the higher the maximum temperature of the combustion chamber, the more heat is transferred to the walls. Exergy heat loss also increases. Fig. 4B shows the temperature of exhaust gases from the engine at different injection times. It is clear that if the injection starts 5 degrees before the top dead point, due to the short heat transfer time and the delay in starting the combustion, the temperature of the exhaust gases has increased significantly. As the ignition start time advances, the time for heat transfer also increases, and the temperature of exhaust gases decreases.

Fig. 4C shows the irreversibility value for different samples. During combustion, due to chemical reactions, entropy production increases, and irreversibility increases significantly. The mentioned figure shows that by the early start of spraying, the amount of irreversibility increases. This is due to an increase in temperature, an increase in the number of chemical reactions and an increase in heat transfer. Fig. 4D shows the exergy of exhaust gases from the engine. The highest exergy of the exhaust gas was observed when the fuel injection began 5 degrees before the top dead center. Advancing the start of fuel injection to 25 degrees before the top dead center resulted in a decrease in this exergy. Conversely, at an injection start time of 35 degrees before the top dead center, the exergy of the exhaust gas increased, attributed to the delayed initiation of the combustion process for that specific sample. The variations in exhaust gas exergy are influenced by the temperature of the exhaust gases from the engine, as represented in Fig. 4C.

Fig. 5 shows the changes in the ignition start time for different injection times. As mentioned, the figure shows that at the injection angle of 35 degrees, the ignition started later, which is the reason for the transfer of heat to the outside. It is worth noting that in this figure, the angle at which 10% of the total cumulative chemical energy of the fuel is released is considered as the ignition start time.

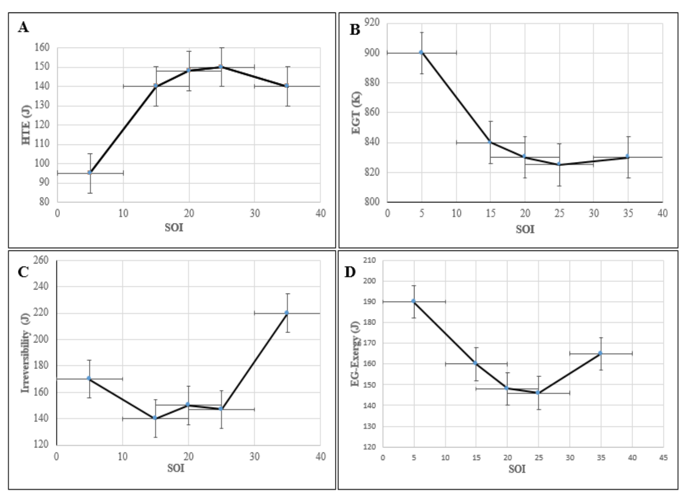

Figure 4. An illustration demonstrating how the timing of the start of injection influences Heat Transfer Exergy (HTE) (A), Exhaust Gas Temperature (EGT) (B), Irreversibility (C), and Exhaust Gas Exergy (EGE) (D).

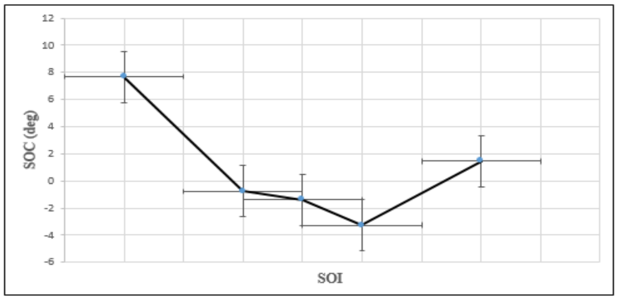

Figure 5. Start of combustion under the effects of the start of injection time (A-form).

Fig. 6 shows the effect of injection time on the production work of the reactive control compression ignition engine. As it is clear in the figure, although the changes in the fuel injection time have led to visible changes in the maximum temperature and pressure inside the chamber, it does not have much effect on the production work of the engine and only in case of injection with a long delay due to incomplete combustion, it causes a reduction in the engine production power.

The outcomes of the first and second laws of thermodynamics are illustrated in Fig. 7. The figure shows that the lowest efficiency of the first and second laws occurred in the case where the fuel injection start time is 5 degrees before the top dead point, which is the reason for the emergence of incomplete combustion.

Fig. 8 demonstrates when the spray is applied during the cycle can affect how much unburned hydrocarbons and carbon monoxide are released. The highest levels of unburned hydrocarbons and carbon monoxide take place during fuel injection at 5 degrees prior to the top dead center due to incomplete combustion. An earlier start to the spray can reduce the amounts of unburned hydrocarbons and carbon monoxide present. It happens due to the temperature inside the cylinder being high and mixed well, resulting in the engine being completely fueled. Ultimately, to determine the conditions that optimize the system's performance, the system's efficiency coefficient has been assessed. The efficiency coefficient is calculated by summing the utilized exergy (such as work) and recoverable exergy including waste heat and exhaust gas exergy, about the overall chemical exergy of the fuels consumed during each cycle.

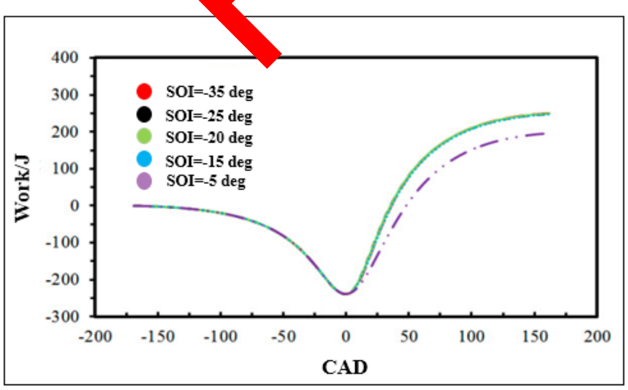

Figure 6. Illustration of the effects of start of injection timing.

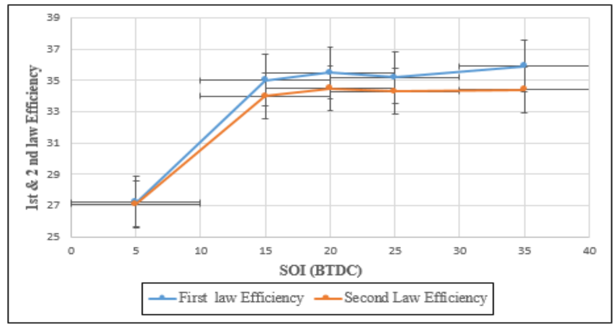

Figure 7. First and second law efficiency under the start of injection timing effects.

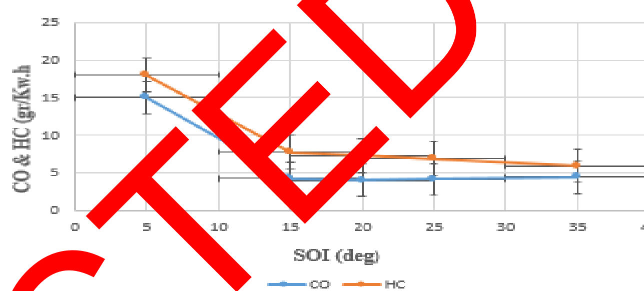

Figure 8. The impact of injection timing on the efficiency factor of the reactive control compression ignition engine.

According to the result in Fig. 9, which is the effects of start of injection timing on utilization factor, by delaying the spraying time too much and by spraying too early, the productivity coefficient decreases. The best efficiency coefficient is observed at the injection angle of 20 degrees before the top dead point. The point to consider in the combustion of compression ignition is reactive control, paying attention to the existing chemical reactions. The engine's emission and performance are mainly controlled through chemical reactions which also play a role in how waste heat is recycled. Table 5 demonstrates the significant chemical events that take place in the combustion chamber at the start of combustion, depending upon the injection time. To investigate the effects of changing the injection time on the chemical processes performed in the reaction control compression combustion engines, the output data from the Converge software was read by a Fortran code, and important reactions were identified using sub-models of the Chem. Kin program.

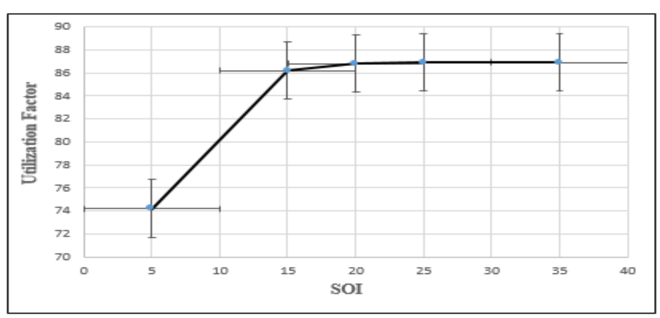

Figure 9. Utilization factors under start of injection timing (case-a).

Table 5. Important reactions inside the combustion chamber at the start of combustion for different injection times.

Injection time -5	Injection time -20	Injection time -35
Methane+ Hydroxide <= > Methyl +Water	Methane+ Hydroxide <= > Methyl +Water	Hydroxide+ Methane<= > Methyl +Water
Oxygen+ Methane<= > Hydroxide+ methyl	Hydrogen +Oxygen+ Nitrogen <= >Hydrogen superoxide +Nitrogen	Oxygen+ Methane<= > Hydroxide+ Methyl
Hydroxide+ Formaldehyde<= >Bicarbonate +Water	Oxygen+ Methane<= > Hydroxide+ Methyl	Hydrogen+2 Oxygen<= > Hydrogen superoxide+ Oxygen
Hydrogen +Oxygen+ Nitrogen <= >Hydrogen superoxide +Nitrogen	Hydrogen +2 Oxygen<= > Hydrogen superoxide+ Oxygen	Hydroxide+ Formaldehyde<= > Bicarbonate+ Water

Table 6 shows the important reactions when 50% of the total chemical energy has been released. According to Table 6, it is clear that the ranking of important reactions for the two samples of spraying time -20 and -35 is very similar. While more different results have been obtained for spraying time -5. The reason for this is the temperature difference of the discussed samples, which has changed the reaction process, and in the -5-degree spray sample, due to the lower temperature, it has been drawn towards reactions with less temperature dependence.

Table 6. Important reactions during the release at crank angle of 50% chemical energy for different spraying times (SOI).

Injection time -5	Injection time -20	Injection time -35
Methane+ Hydroxide <= > Methyl +Water	Hydroxide+ Methane <= > Methyl+ Water	Hydroxide+ Methane<= > Methyl+ Water
Hydroxide+ Formaldehyde<= >Hydrogen carbonate +Water	Oxygen+Hydrogen+2 Hydroxide<= > Hydroxide + Hydroxide	Oxygen+Hydrogen+2 Hydroxide<= > Hydroxide + Hydroxide
Methyl+ Bicarbonate =Formaldehyde +Methylene	Hydroxide+ Hydrogen peroxide<= >Hydroperoxyl+ Water	Hydroxide+ hydrogen peroxide <=>
Methanol=Methoxide+ Hydroxide	Hydroxide+ Formaldehyde<= >Bicarbonate+ Water	Hydroxide+ Formaldehyde<=>Bicarbonate+ Water
Oxygen +Methane<= > Hydroxide+ Methyl	Hydr[illegible]e+ [illegible]<= >Hydroperoxyl+ Water	Hydrogen+ Oxygen+ Water<=> Hydroperoxyl+Water

It is worth mentioning that the ranking of the reactions has been done according to the progress rate of the reactions in terms of moles per cubic centimeter per second. According to the two mentioned tables, it can be concluded that time changes the course of reactions.

In this study, a valid computational fluid dynamics model was used to investigate the effect of injection start time in a reactive control compression ignition engine on the capacity of recycled wasted heat. The data calculated by the computational fluid dynamics model were called by a mathematical model and used to calculate different exergy values. The results obtained indicate that initiating fuel injection earlier allows for a longer period for fuel and air to mix, resulting in more complete combustion and a reduction in the emissions of unburned hydrocarbons and carbon monoxide. Moreover, with earlier injection start times, the higher temperatures in the combustion chamber lead to greater exergy in heat transfer due to enhanced heat exchange, which also contributes to a decrease in the exhaust gas temperature from the engine. Additionally, the elevated temperature associated with earlier injection timing increases the irreversibility owing to a rise in chemical reaction rates. Additionally, the findings indicated that moving the fuel injection timing forward enhances both the second law of thermodynamics efficiency and the overall system efficiency. This adjustment also increases the capacity for waste heat recovery within the system. Based on the results obtained, it is evident that the reactive control compression ignition engine, when the injection begins 20 degrees before top dead center, exhibits the greatest second-law efficiency, the highest work output, the best productivity ratio, and the least amount of pollution. At injection angles earlier than this optimal setting, increased heat transfer leads to higher pollution levels, while later injection timings result in inadequate mixing of the fuel and air, causing higher emissions and reduced efficiency ratios.

4. Conclusion

In conclusion, based on the current research, the high temperature has caused the irreversibility to increase due to the increase in the number of chemical reactions. Furthermore, the efficiency of the system increased with advanced fuel injection start time.

Funding: This research received no external funding.

Data Availability Statement: The datasets used during the current study are available from the corresponding author on reasonable request.

Ethical Statement: This research adheres to the ethical guidelines established by the Committee on Publication Ethics (COPE). All procedures and methodologies used in this study comply with COPE standards, ensuring transparency, integrity, and respect for all participants involved.

Conflicts of Interest: The authors declare no conflict of interest.

References

[1] D. Thombare and C. Copeland, "Review on Exhaust Gas Heat Recovery for I . C . Engine Related papers Review on Exhaust Gas Heat Recovery for I . C . Engine," vol. 2, no. January 2013, pp. 93–100, 2018.

[2] H. Tian, P. Liu, and G. Shu, "Challenges and opportunities of Rankine cycle for waste heat recovery from internal combustion engine," Prog. Energy Combust. Sci., vol. 84, p. 100906, 2021.

[3] R. Saidur, M. Rezaei, W. K. Muzammil, M. H. Hassan, S. Paria, and M. Hasanuzzaman, "Technologies to recover exhaust heat from internal combustion engines," Renew. Sustain. Energy Rev., vol. 16, no. 8, pp. 5649–5659, 2012.

[4] A. T. Hoang, "Waste heat recovery from diesel engines based on Organic Rankine Cycle," Appl. Energy, vol. 231, no. September, pp. 138–166, 2018.

[5] A. A. Manzela, S. M. Hanriot, L. Cabezas-Gómez, and J. R. Sodré, "Using engine exhaust gas as energy source for an absorption refrigeration system," Appl. Energy, vol. 87, no. 4, pp. 1141–1148, 2010.

[6] M. Talbi and B. Agnew, "Energy recovery from diesel engine exhaust gases for performance enhancement and air conditioning," Appl. Therm. Eng., vol. 22, no. 6, pp. 693–702, 2002.

[7] M. Kumar and R. K. Das, "Experimental Analysis of Absorption Refrigeration," vol. 23, no. 1, pp. 149–157, 2019.

[8] A. Abusoglu and M. Kanoglu, "First and second law analysis of diesel engine powered cogeneration systems," Energy Convers. Manag., vol. 49, no. 8, pp. 2026–2031, 2008.

[9] K. K. Srinivasan, P. J. Mago, and S. R. Krishnan, "Analysis of exhaust waste heat recovery from a dual fuel low temperature combustion engine using an Organic Rankine Cycle," Energy, vol. 35, no. 6, pp. 2387–2399, 2010.

[10] B. Alizadeh Kharkeshi, R. Shafaghat, S. Talesh Amiri, A. M. Tahan, and A. Ardebilipour, "Effect of Diesel-engine Operating Conditions on Performance of Waste Heat Recovery Cycles: A 4E Analysis," Iran. J. Energy Environ., vol. 15, no. 3, pp. 220–234, 2024.

[11] V. P. and D. Deshmukh, "A comprehensive review of waste heat recovery from a diesel engine using organic rankine cycle," Energy Reports, vol. 7, pp. 3951–3970, 2021.

[12] F. Yang et al.., "Performance analysis of waste heat recovery with a dual loop organic Rankine cycle (ORC) system for diesel engine under various operating conditions," Energy Convers. Manag., vol. 80, pp. 243–255, 2014.

[13] J. B. Obi, "State of art on ORC applications for waste heat recovery and micro-cogeneration for installations up to 100kWe," Energy Procedia, vol. 82, pp. 994–1001, 2015.

[14] M. H. Yang and R. H. Yeh, "Analyzing the optimization of an organic Rankine cycle system for recovering waste heat from a large marine engine containing a cooling water system," Energy Convers. Manag., vol. 88, pp. 999–1010, 2014.

[15] E. Açikkalp, H. Aras, and A. Hepbasli, "Advanced exergoeconomic analysis of a trigeneration system using a diesel-gas engine," Appl. Therm. Eng., vol. 67, no. 1–2, pp. 388–395, 2014.

[16] M. Z. Márton Virt, "Realization of Low Temperature Combustion in an Unmodified Diesel Engine." Cognitive Sustainability, p. 3(2), 2024.

[17] M. Krishnamoorthi, R. Malayalamurthi, Z. He, and S. Kandasamy, "A review on low temperature combustion engines: Performance, combustion and emission characteristics," Renew. Sustain. Energy Rev., vol. 116, no. February, p. 10[illegible]404, 20[illegible].

[18] A. K. Agarwal, A. P. Singh, and R. K. Maurya, "Evolution, challenges and path forward for low temperature combustion engines," Prog. Energy Combust. Sci., vol. 61, pp. 1–56, 2017.

[19] N. Sarabchi, R. Khoshbakhti Saray, and S. M. S. Mahmoudi, "Utilization of waste heat from a HCCI (homogeneous charge compression ignition) engine in a tri-generation system," Energy, vol. 55, pp. 9[illegible]–976, 2013.

[20] M. Khaljani, R. K. Saray, and K. Bahlouli, "Evaluation of a combined cycle based on an HCCI (Homogenous Charge Compression Ignition) engine heat recovery employing two organic Rankine cycles," Energy, vol. 107, pp. 748–760, 2016.

[21] A. Paykani, A. Garcia, M. Shahbakhti, P. Rahnama, and R. D. Reitz, "Reactivity controlled compression ignition engine: Pathways towards commercial viability," Appl. Energy, vol. 282, no. PA, p. 116174, 2021.

[22] G. Szamrej, M. Karczewski, and J. Chojnowski, "A review of technical solutions for rcci engines," Combust. Engines, vol. 189, no. 2, pp. 36–46, 2022.

[23] M. Anish et al.., "Impact of reactivity controlled compression ignition (RCCI) mode engine operation in diesel engine powered with B20 blend of waste cooking oil biodiesel," Sci. Rep., vol. 13, no. 1, pp. 1–15, 2023.

[24] Y. Li, M. Jia, Y. Chang, and G. Xu, "Comparing the Exergy Destruction of Methanol and Gasoline in Reactivity Controlled Compression Ignition (RCCI) Engine," SAE Tech. Pap., vol. 2017-March, no. March, 2017.

[25] D. Liu, H. Wang, H. Liu, Z. Zheng, Y. Zhang, and M. Yao, "Identification of factors affecting exergy destruction and engine efficiency of various classes of fuel," Energy, vol. 211, p. 118897, 2020.

[26] M. Mohebbi, M. Reyhanian, V. Hosseini, M. F. Muhamad Said, and A. A. Aziz, "Performance and emissions of a reactivity controlled light-duty diesel engine fueled with n-butanol-diesel and gasoline," Appl. Therm. Eng., vol. 134, pp. 214–228, 2018.

[27] X. Liu, H. Wang, Z. Zheng, and M. Yao, "Development of a reduced primary reference fuel-PODE3-methanol-ethanol-n-butanol mechanism for dual-fuel engine simulations," Energy, vol. 235, 2021.

[28] K. Poorghasemi, R. K. Saray, E. Ansari, B. K. Irdmousa, M. Shahbakhti, and J. D. Naber, "Effect of diesel injection strategies on natural gas/diesel RCCI combustion characteristics in a light duty diesel engine," Appl. Energy, vol. 199, pp. 430–446, 2017.

[29] A. K. Amjad, R. Khoshbakhti Saray, S. M. S. Mahmoudi, and A. Rahimi, "Availability analysis of n-heptane and natural gas blends combustion in HCCI engines," Energy, vol. 36, no. 12, pp. 6900–6909, 2011.

[30] C. Böhringer and N. Rivers, "The energy efficiency rebound effect in general equilibrium," J. Environ. Econ. Manage., vol. 109, no. June 2020, p. [illegible]02508, 2021.

[31] K. Weigel-Milleret and W. Grzegozek, "Modelling and simulation of narrow car dynamic," IOP Conf. Ser. Mater. Sci. Eng., vol. 421, no. [illegible], 2018.

[32] M. Kircher et al.., "Investigation of Engine Combustion and Auto-ignition of a Multicomponent Surrogate Fuel with NTC Behavior Under Knocking Conditions," Flow, Turbul. Combust., vol. 110, no. 1, pp. 149–169, 2023.

[33] P. J. O'Rourke and A. A. Amsden, "The Tab Method for Numerical Calculation of Spray Droplet Breakup International Fuels and Lubricants Meeting and Exposition Toronto, Ontario," SAE Tech. Pap. Ser., vol. 872089, p. 12, 1987.

[34] [illegible] Kobashi, Y. Zama, and T. Kuboyama, "Modeling wall film formation and vaporization of a gasoline surrogate fuel," Int. J. Heat Mass Transf., vol. 147, p. 119035, 2020.

[35] V. Yakhot, S. A. Orszag, S. Thangam, T. B. Gatski, and C. G. Speziale, "Development of turbulence models for shear flows by a double expansion technique," Phys. Fluids A, vol. 4, no. 7, pp. 1510–1520, 1992.

[36] S. Barrier, "A temperature wall function formulation for variable-density turbulent flows with application to engine convective heat transfer modeling," Int. heat mass Transf., vol. 40, no. 1, pp. 1–7, 2005.

[37] S. Jafarmadar and N. Javani, "Exergy analysis of natural gas/DME combustion in homogeneous charge compression ignition engines (HCCI) using zero-dimensional model with detailed chemical kinetics mechanism," Int. J. Exergy, vol. 15, no. 3, pp. 363–381, 2014.

[38] S. Jafarmadar and P. Nemati, "Exergy analysis of diesel/biodiesel combustion in a homogenous charge compression ignition (HCCI) engine using three-dimensional model," Renew. Energy, vol. 99, pp. 514–523, 2016.

[39] C. D. Rakopoulos, M. A. Scott, D. C. Kyritsis, and E. G. Giakoumis, "Availability analysis of hydrogen/natural gas blends combustion in internal combustion engines," Energy, vol. 33, no. 2, pp. 248–255, 2008.